Mode II Fracture Mechanisms of PBT-Modified Brittle Epoxies

HO SUNG KIM, PYO MA

Department of Mechanical Engineering, The University of Newcastle, Callaghan, NSW 2308, Australia

Received 4 June 1997; accepted 1 November 1997

ABSTRACT: Mode II fracture behavior of poly(butylene terephthalate) (PBT)-modified epoxy systems are studied. Two different types of testing for mode II fracture are conducted. One was to investigate the fracture behavior of bulk epoxy systems, in comparison with mode I fracture, using single-edge notched specimens under skew symmetric four-point loading. The other was to investigate the fracture behavior of epoxy layers sandwiched between aluminium adherends using compact shear specimens. The mode II fracture toughness obtained from the former for modified systems has been found to increase significantly over the control, although the increase of mode I fracture toughness for modified systems over the control is moderate. This finding is discussed in relation with cavitation and equivalent mode I stress intensity factor and also in comparison with rubber-modified epoxy systems in the literature to account for the increase. In addition, the difference in fracture morphology between mode I and II is discussed. Mode II fracture toughness obtained from the latter for modified systems has also been found to increase significantly over the control. Morphology of fracture surfaces relating to this finding is discussed. © 1998 John Wiley & Sons, Inc. J Appl Polym Sci 69: 405–415, 1998

Key words: mode II; fracture; toughening; epoxy; adhesive

INTRODUCTION

Toughened epoxies are widely used as structural adhesives and matrices of fiber-reinforced composites in various industries. For toughening of epoxies, rubber has been used as a modifier, but an increase in toughness is achieved at the expense of other properties, such as elastic modulus and yield strength.[1] An alternative approach to toughen the epoxies is to employ thermoplastics as modifiers. Such thermoplastic modifiers used by investigators include polysulfone (PSF), poly(ether ketone) (PEK), poly(ether sulfone) (PES), poly(ether imide) (PEI), poly(phenylene oxide) (PPO), poly(carbonate) (PC), poly(butylene terephthalate) (PBT), and some copolymers. The details of these modifies are reviewed elsewhere.[2]

PBT has been known as one of successful thermoplastic modifiers in increasing toughness.[3] Mechanisms responsible for the increase in mode I fracture toughness include crack bridging, crack bifurcation, and ductile fracture of PBT particles. In addition, phase transformation was thought to be the major toughening mechanism, but it was inconclusive. In applications in which mode II loading is involved, such as adhesives in a lap joint and matrices of fiber-reinforced composites subjected to delamination, mode II fracture mechanisms are of interest. However, the study on the fracture mechanisms has been confined to those of mode I, although the mechanism of mode II fracture has been known to be different from that of mode I fracture.[4,5]

There is difference in stress field around crack tip between modes I and II.[6] Accordingly, the di-

Correspondence to: H. S. Kim.

Journal of Applied Polymer Science, Vol. 69, 405–415 (1998)
 CCC 0021-8995/98/020405-11

rection of crack propagation depends on the loading mode. It has been known that the crack propagation under mode II loading is driven by the major principal stress, and its resulting fracture is essentially of mode I.[6–8] However, Kim and Ma[5] recently demonstrated that fracture initiation of brittle epoxy systems under mode II loading is, in fact, of mode II. They showed that a band of sliding marks along the line of crack tip was formed. In mode II fracture, accordingly, fracture mechanisms are expected to be affected by more shear deformation than in mode I fracture. The main purpose of this work was to investigate mechanisms of mode II fracture for PBT-modified epoxy systems using both unconstrained bulk specimens and constrained layers between aluminium adherends.

EXPERIMENTAL DETAILS

Materials

The resin employed was a diglycidyl ethers of bisphenol A (DGEBA)-based epoxy (GY260, Ciba-Geigy) cured using 4,4′ diaminodiphenyl sulphone (DDS). Poly(1,4-butylene terephthalate) (PBT) was used for modifications. The PBT (Aldrich Chemical Co., Castle Hill, Australia) was in the form of pellets, and it was characterized elsewhere[9] as having a molar mass of 37,800 and a nominal melting temperature of 227°C. The PBT pellets were processed into particulate form by dissolution for the use as modifier.

The process for preparation of PBT particles is as follows: PBT pellets were mixed with liquid epoxy, and the mixture was placed in an oven preheated at 230°C; slow stirring (for 1 h) was followed until it became clear, indicating that the PBT is dissolved; and the mixture was cooled down to room temperature for precipitation in acetone and then washed with acetone until it became white. The particles were dried at 30°C in an oven for 24 h. The distribution of particle size obtained using a Malvern 2600 droplet and particle size analyzer is shown in Figure 1. The particles were separated using a sieve with an aperture of 500 μm.

The processing for PBT particle-modified epoxy–DDS systems was as follows: sieved PBT particles were mixed with epoxy, and this mixture was placed and held for 1 h in an oven preheated at 200°C until it became clear; the mixture was taken out of the oven to add DDS and to be degassed under vacuum; and this mixture was placed back in oven at 135°C until DDS was completely dissolved. The resin system was poured into a mold and subsequently cured for 24 h at 120°C, followed by 4-h postcure at 180°C. It was allowed to cool down slowly in oven (about 10 hours). The control epoxy system was prepared in the same way, but without PBT.

Preliminary tests for different processing of PBT-modified epoxy were conducted. In this process, PBT particles (20 phr by weight) were directly mixed with curing agent and epoxy at room temperature and followed by the standard curing schedule, excluding the initial step for 200°C heating, described above. However, properties such as modulus and toughness were not improved, and flexural strength was even significantly decreased. This process was not proceeded any further.

Mechanical Tests

Molded sheets of different epoxy systems, 6 mm thick, were cut into specimens for flexural and fracture tests. At least 3 specimens were used for each PBT content. All the tests were conducted at 23°C and at a crosshead speed of 1 mm/min, unless otherwise specified. Flexural moduli and strengths were obtained using a four-point bending rig in accordance with ASTM D790M-92. The following three different ways of fracture tests for epoxy systems were conducted: three-point bend test for mode I, skew symmetric four-point shear test for mode II, and compact shear test for mode II of epoxy layers sandwiched between 6060-T5 aluminium adherends.

Yield stress of brittle materials is difficult to measure in a tensile test because of its premature failure before the gross yielding is reached. Therefore, compressive yield stress and crush stress were measured using a jig shown in Figure 2. The width of steel dies is 8 mm. Broken specimens already used for skew symmetric four-point test for mode II were reused for the compression tests. Four specimens were used for each PBT content. Thickness and width of specimen is 6 and 10 mm, respectively, and, therefore, the initial contact area between dies and specimen is 8×10 mm. True stress was estimated using intermittent measurements of testpiece dimensions during the test for a linear extrapolation for true area. The true strain was calculated using

$$\varepsilon = \ln \frac{B}{B_0} \tag{1}$$

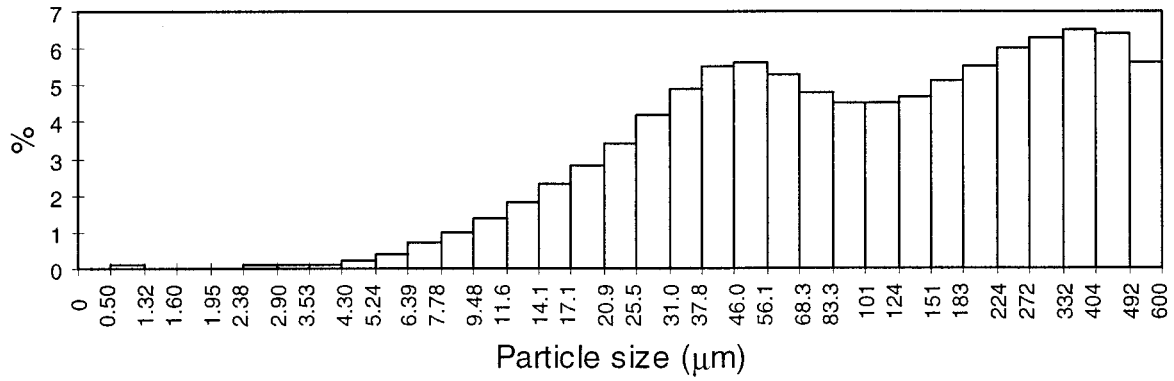

Figure 1 Size distribution of PBT particles before sieving.

where ε is the true strain, B is the thickness, and the subscript 0 denotes initial.

For the fracture tests of mode I and four-point mode II, a precrack was produced by tapping a razor blade at the tip of mechanical notch on each specimen. The three-point bend tests for mode I fracture toughness were conducted in accordance with ASTM D5045-91a. The following expression for the critical stress intensity factor, K_{IC}, was used for calculations of fracture toughness for mode I:

$$K_{IC} = \frac{P_Q}{B\sqrt{W}} \times \left(\frac{\sqrt[6]{\frac{a}{W}}\left[\left(1.99 - \left(\frac{a}{W}\right)\left(1 - \left(\frac{a}{W}\right)\right)\right) \times \left(2.15 - 3.93\left(\frac{a}{W}\right) + 2.7\left(\frac{a}{W}\right)^2\right)\right]}{\left[1 + 2\left(\frac{a}{W}\right)\right]\left[1 - \left(\frac{a}{W}\right)\right]^{3/2}} \right) \quad (2)$$

where P_Q is the critical fracture load, which in the current study corresponds to the maximum load; B is the thickness; W (= support span/4) is the width; and a is the crack length.

The skew symmetric four-point shear tests for mode II fracture toughness were conducted at a crosshead speed of 0.5 mm/min (Fig. 3). The following expression was used for calculations of mode II fracture toughness [10]:

$$K_{IIC} = \tau Y \sqrt{a} \quad (3)$$

where $\tau\{= [\beta - \alpha)F/(\alpha + \beta)]/BW\}$ is the shear stress, and Y is a function of a/W given by

$$Y = \sqrt{\pi} \frac{\left[1.122 - 0.561\left(\frac{a}{W}\right) + 0.085\left(\frac{a}{W}\right)^2 + 0.18\left(\frac{a}{W}\right)^3\right]}{\sqrt{1 - \left(\frac{a}{W}\right)}} \quad (4)$$

For mode II fracture toughness measurements

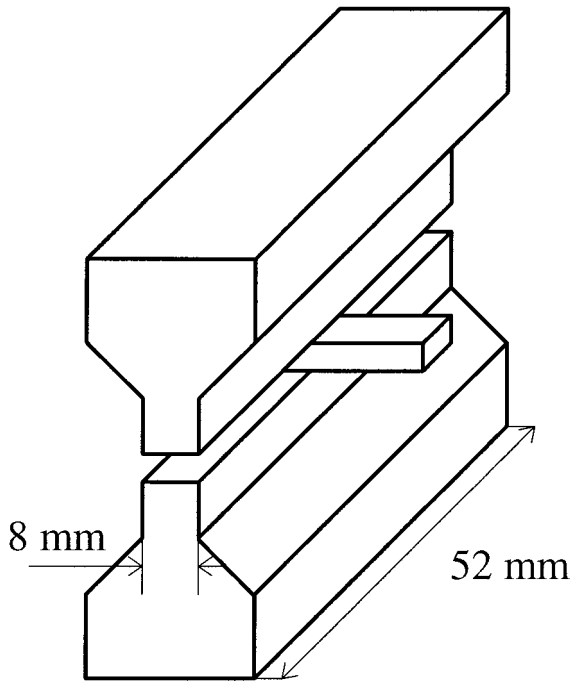

Figure 2 Jig used for compressive tests.

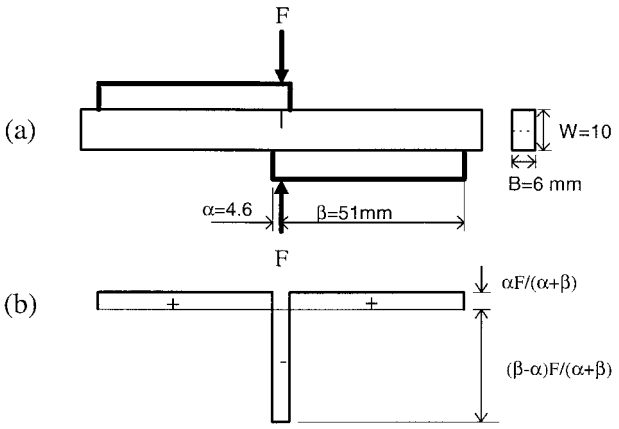

Figure 3 (a) Dimensions of specimen and skew symmetric four-point loading for mode II fracture. (b) Shear force diagram.

for epoxy layers sandwiched between 6060-T5 aluminium adherends (Fig. 4), at least 3 specimens were used for each PBT content. The test setup is schematically shown in Figure 5. The aluminium bonding surfaces were sanded with 320-grit silicon carbide sandpaper manually, followed by degreasing with acetone, rinsing thoroughly with tap water, and drying in an oven. A razor blade for a paint scraper with an average thickness of 0.26 mm was used as a spacer between aluminium adherends, and its cutting edge was used for molding the initial crack tip in the bond line. The razor blade was coated with a releasing agent. This procedure with razor blades for preparing

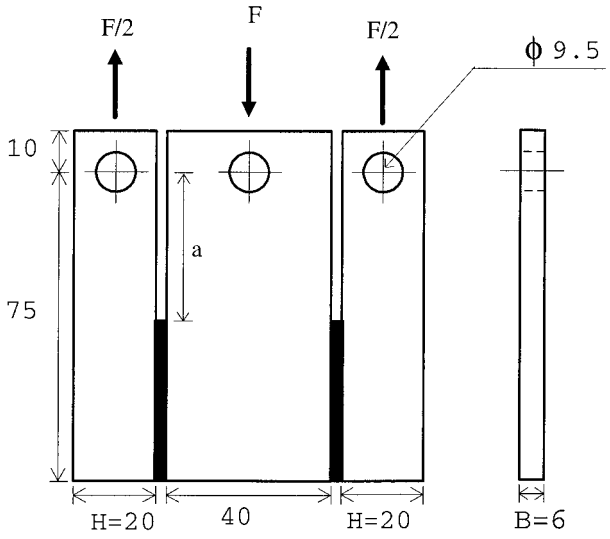

Figure 4 Compact shear specimen for epoxies sandwiched between 6060-T5 aluminium adherends (dimensions are in mm).

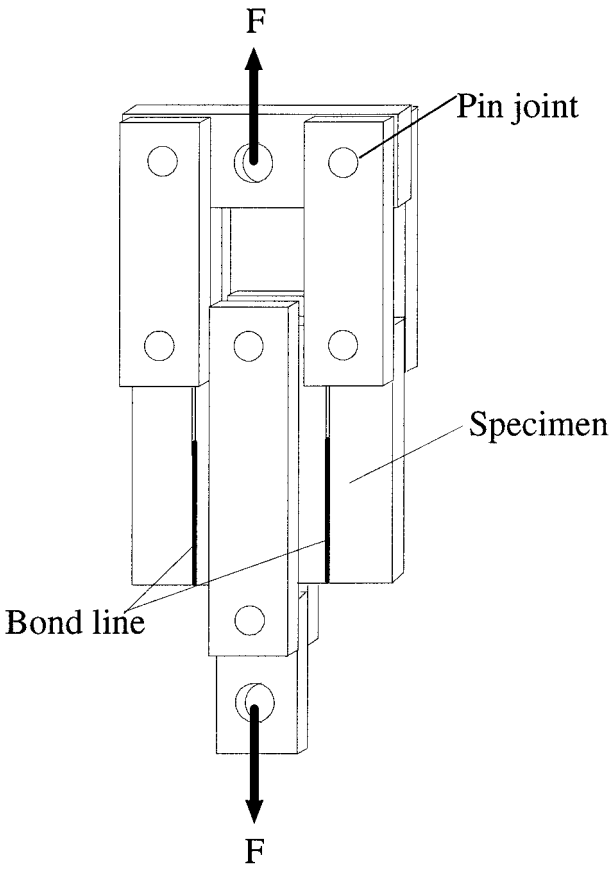

Figure 5 Test setup for mode II fracture using compact shear specimen.

crack tips of adhesive joints had been found to be more efficient than using Teflon tapes or releasing agent. Spacers and adherends were secured with heat-resistant tapes to form cavities for adhesive layers. The following expression was used for the calculation of mode II fracture toughness of the adhesive layer[11]:

$$K_{IIC} = \frac{P_Q}{BH}\sqrt{a}\left(\frac{E_{ep}}{E_{al}}\right)^{1/2} \qquad (5)$$

where P_Q is the critical fracture load, which, in the current study, corresponds to the maximum load; H is the width (see Fig. 4); and E_{ep} and E_{al} are the elastic moduli of epoxy and aluminium, respectively. Note that if the calculation is conducted according to the numerical result given by Anandarajah,[12] the values of K_{IIC} are about 13% lower for the given dimensions and properties than those calculated according to eq. (5).

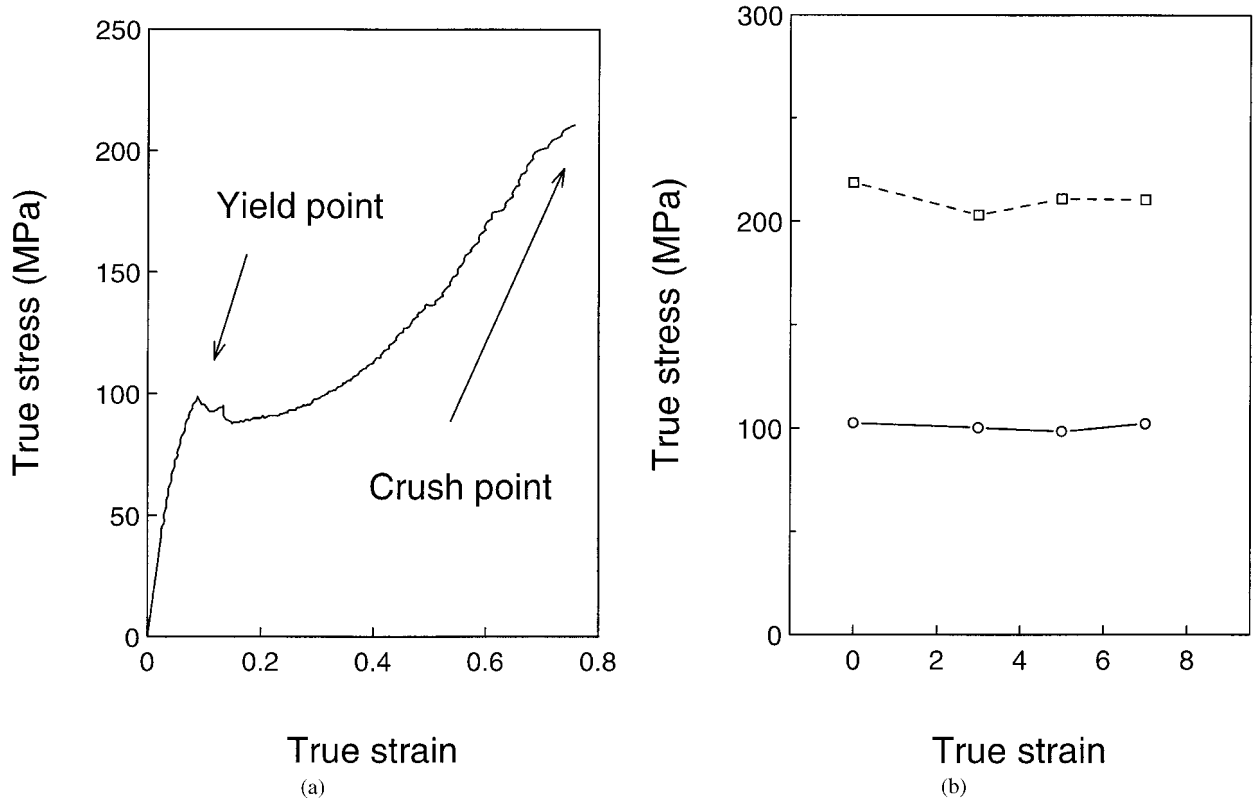

Figure 6 (a) A typical compressive stress–strain curve at a PBT content of 5 phr. (b) A plot of (○) compressive yield stress and (□) crush stress as a function of PBT content.

RESULTS AND DISCUSSION

Mechanical Properties and Mode I Fracture

A typical compressive stress–strain curve is shown in Figure 6(a), and yield and crush stresses are plotted as a function of PBT content in Figure 6(b). Yield stress appears to be independent of PBT content, while crush stress (or compressive strength) increases slightly with the increasing PBT content. Also, other properties, such as flexural modulus and flexural strength, were obtained as part of characterization of epoxy systems. Flexural modulus, as shown in Figure 7(a), is more or less independent of rubber content, but flexural strength decreases significantly as the PBT content increases, as shown in Figure 7(b).

The effect of PBT modification on mode I fracture toughness of bulk epoxies is given in Figure 8 and also in Table I. Some moderate improvement on the fracture toughness is exhibited. At a PBT content of 3 phr, there is an increase of 21% on the control; but at higher PBT content, only a slight further increase accounting for 26% at 7 phr is found.

In a preliminary test with double U-notched specimens for examination of permanent deformation due to triaxial stress,[13,14] it was found that there is no stress-whitening at the root of U-notch in an epoxy system modified with a PBT content of 5 phr, indicating that there is no cavitation-induced deformation in the matrix.

Morphology of fracture surfaces of PBT-modified epoxy systems was characterized mainly by tailing in the wake of PBT agglomerates of small diameter particles and by unclear interface between particles and matrix. These features are similar to those obtained by one of processes for PBT-modified epoxy systems by other investigators.[15] The tailing is evidence for a crack-pinning mechanism, which can be a major source of toughening in rigid particle-filled epoxies.[1,16] Figure 9 exemplifies the morphology of such a fracture surface at a PBT content of 3 phr. At a higher magnification [Fig. 9(b)], clam-shaped fracture surfaces between agglomerates are seen. Mode I

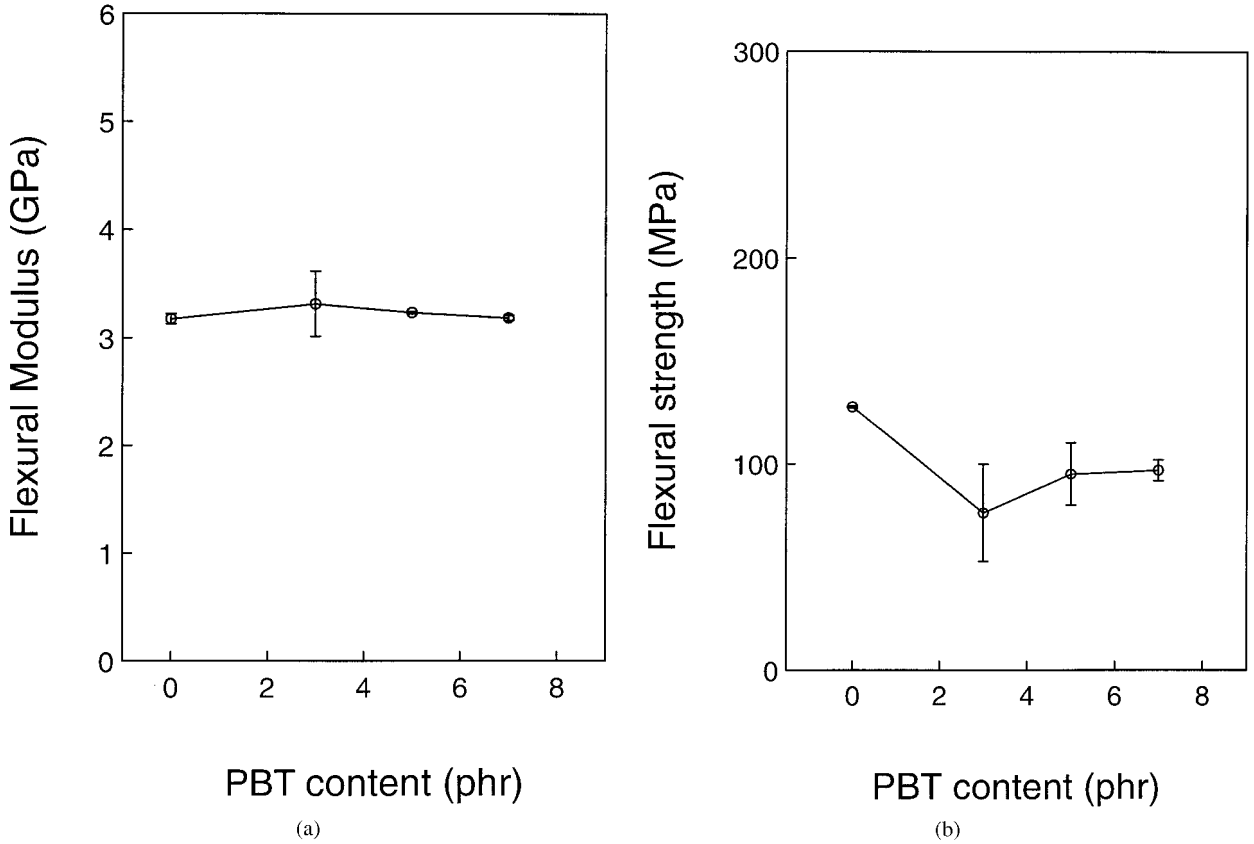

Figure 7 Flexural properties as a function of PBT content, obtained from four-point bend tests: (a) flexural modulus; (b) flexural strength.

toughening mechanisms and processing of PBT-modified epoxy systems have already been investigated.[3,9,15,17] Therefore, it is not our intention to investigate mode I mechanisms further but to investigate mode II fracture behavior with reference to that of mode I.

Mode II Fracture of Bulk Epoxy Systems Under Skew Symmetric Four-Point Loading

Mode II fracture toughness of bulk epoxies was obtained under skew symmetric four-point loading and is given in Figure 10 and listed in Table I as a function of PBT content. The toughness generally increases with the addition of PBT. This finding is in contrast with that of rubber-modified epoxy systems[5] in which the mode II fracture toughness decreases with increasing rubber content. There are differences between rubber[13] and PBT modifiers in these epoxy systems. One is in the capability of cavitation due to triaxial stress. Rubber particles cavitate in mode I fracture, but PBT particles do not. This differences would be an advantage for PBT-modified epoxies over rubber-modified epoxies in mode II fracture because there would not be a loss of toughness due to cavitation when fracture changes from mode I and mode II. Another difference is in deformability. No marks for shear deformation on the fracture surface in the vicinity of crack tip in PBT-modified systems were found. However, rubber-modified epoxies have sliding marks at the initiation of crack propagation under mode II loading, indicating that crack initiation is due mainly to shear stress, although some cavitation was observed as well within sliding marks.[5] A further difference is that PBT particles are rigid compared to rubber particles. Accordingly, it is deduced that PBT particles are obstacles at crack initiation more to shear deformation in the maximum shear plane than to mode I crack propagation due to the major principal stress. Then, the crack initiation would prefer to be governed by the maximum principal stress, resulting that no shear deformation marks were generated in PBT-modified epoxy systems.

The initial crack extension angle to the maxi-

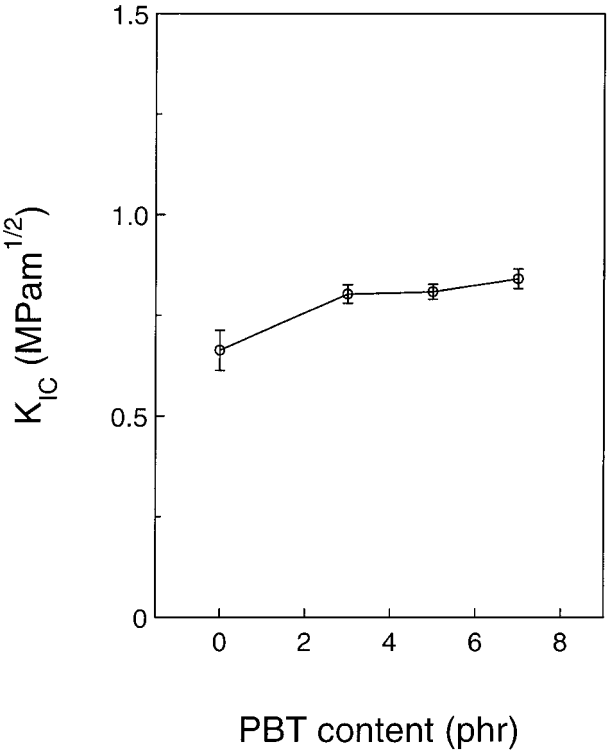

Figure 8 Mode I fracture toughness versus PBT content, obtained from three-point bend tests.

mum shear plane for each PBT content was measured and is shown in Table II. Measured values are in reasonable agreement with the theoretical value of −70.5° obtained from the principal stress criterion.[7] This allows for calculation of the equivalent mode I fracture toughness, K_{ICeq}, using the following expression[6]:

$$K_{ICeq} = K_I \cos^3 \frac{\theta_m}{2} - 3K_{II} \cos^2 \frac{\theta_m}{2} \sin \frac{\theta_m}{2}$$
$$= -3K_{IIC} \cos^2 \frac{-70.5°}{2} \sin \frac{-70.5°}{2} \quad (6)$$

Table I Fracture Toughness Measured (K_{IC}, K_{IIC}) and Calculated (K_{ICeq}) for Bulk Epoxies

PBT Content (phr)	K_{IC} (MPa m$^{1/2}$)	K_{ICeq} (MPa m$^{1/2}$)	K_{IIC} (MPa m$^{1/2}$)
0	0.66 ± 0.05	0.93	0.81 ± 0.33
3	0.80 ± 0.02	1.54	1.34 ± 0.21
5	0.81 ± 0.02	1.67	1.45 ± 0.13
7	0.84 ± 0.03	1.47	1.28 ± 0.3

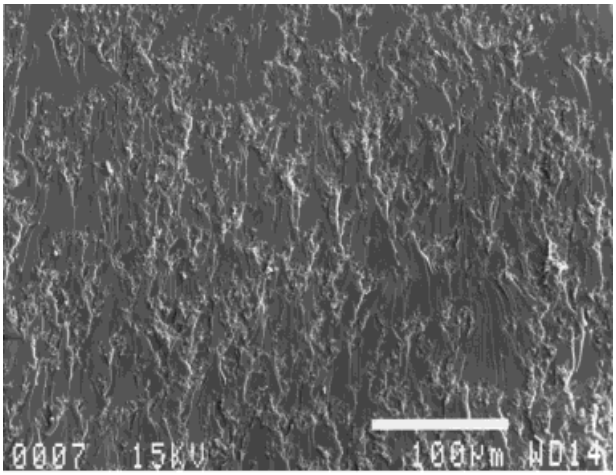

(a)

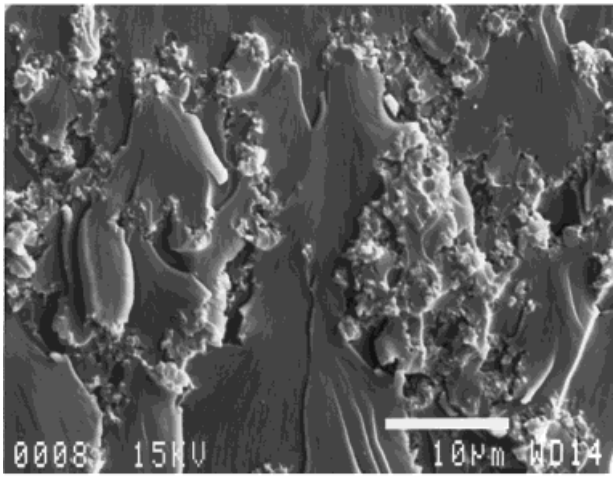

(b)

Figure 9 Morphological features of mode I fracture surface at a PBT content of 3 phr at (a) a low magnification and (b) a high magnification. The crack propagation direction is from top to bottom.

where θ_m is the crack extension angle. The values of K_{ICeq} are listed in Table I. It is noted that the values of K_{ICeq} are much higher than those of K_{IC}, particularly for modified systems.

Fracture surfaces were examined using a scanning electron microscope (SEM). There are some differences in fracture surface characteristics of modified systems between mode I and mode II loading. One of differences is that those under mode II loading had some ridges originating from the initial crack tip for both modified systems and the control, whereas those under mode I loading are flat, as is shown in Figure 9. This difference is due to the fact that new cracks under mode II loading are likely to initiate on slightly different planes because the initial starter crack is not per-

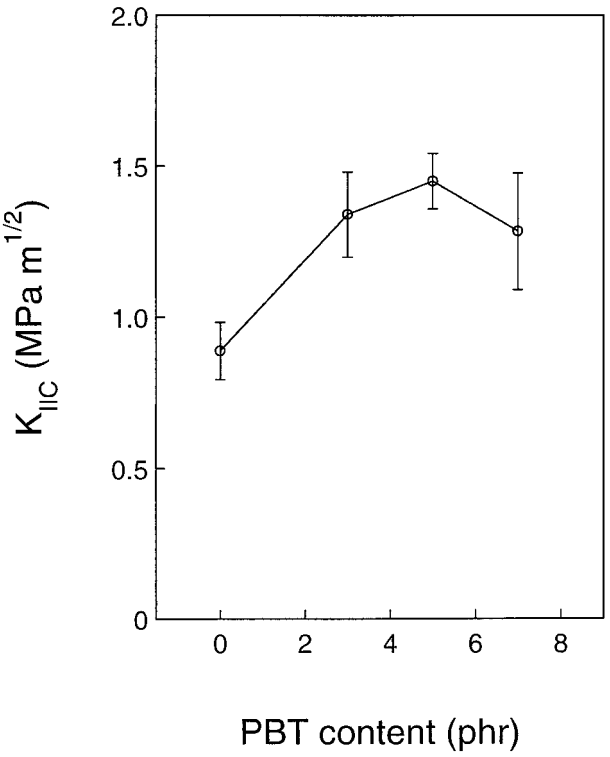

Figure 10 Mode II fracture toughness of bulk epoxy versus PBT content, obtained under skew symmetric four-point loading.

fectly uniform and straight.[4] Figure 11 shows such features generated under mode II loading at a PBT content of 3 phr. Another difference is that fracture surfaces of PBT-modified systems generated under mode II loading are largely scaly (Fig. 11), although some features are partly similar to those generated under mode I loading, as shown in Figure 12. These differences in fracture surfaces seem to relate to the fact that the values of K_{ICeq} are higher than those of K_{IC}. The former seems to contribute to the increase in K_{ICeq} for both modified and control systems. The latter seems to add additional increase for modified systems.

Figure 13 shows that the control has a band of

Table II Measured Crack Extension Angles of Bulk Exposies under Mode II Loading

PBT Content (phr)	Crack Extension Angle (deg)
0	−63.00
3	−72.17
5	−67.17
7	−62.50

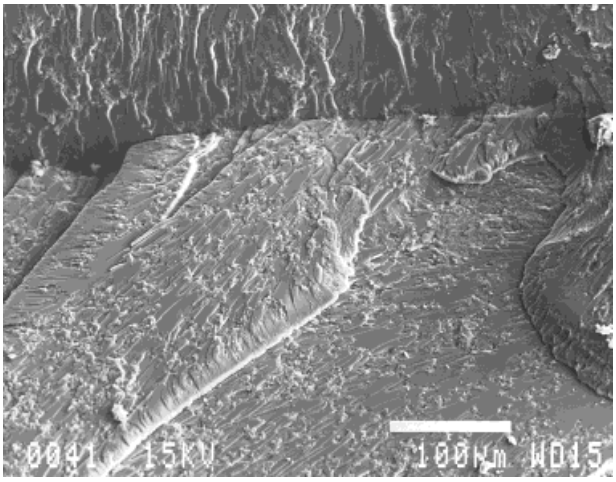

Figure 11 Morphological features of mode II fracture surface at a PBT content of 3 phr under skew symmetric four-point loading. It is seen that ridges are originated from the initial crack tip, and its surface is scaly. The crack propagation direction is from top to bottom.

sliding marks ahead of initial crack tip, unlike modified systems.

Fracture of Adhesive Layers Sandwiched Between Aluminium Adherends

The effect of PBT modification on the fracture toughness of adhesive layer sandwiched between 6060-T5 aluminium adherends is shown in Figure 14 as a function PBT content. At a small amount of PBT content (3 phr), the toughness increases

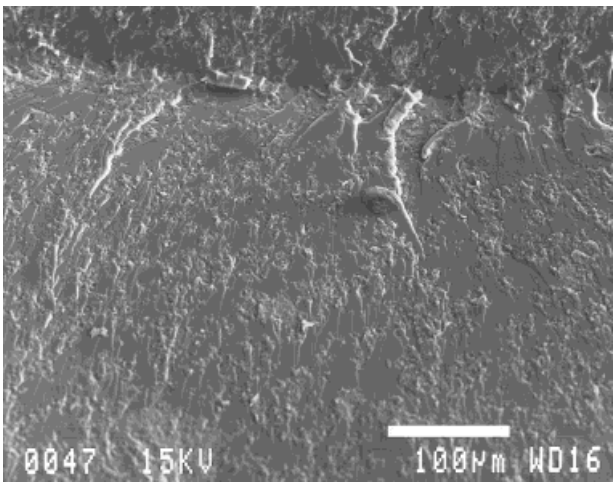

Figure 12 Morphological features of mode II fracture surface at a PBT content of 5 phr under skew symmetric four-point loading. It is seen that its features resemble those of mode I.

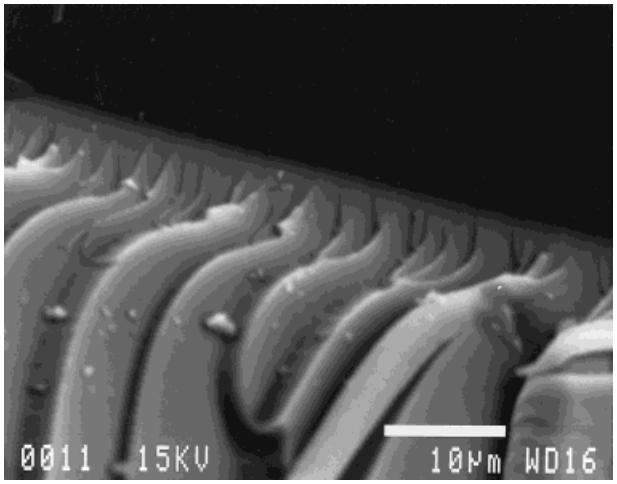

Figure 13 Morphological features of control mode II fracture surface under skew symmetric four-point loading. A band of sliding marks is formed along the initial crack tip. The dark area in the top is the precrack.

by 49% over the control, although any further increases were not achieved at higher PBT contents.

In the first instance, fracture surfaces were examined visually without the aid of a microscope. The fracture of the control was found to be dominantly interfacial, and its surfaces on the adhesive side contained multiple tunnelling[18–21] of microcracks across the thickness of the specimen. In contrast, PBT-modified epoxy systems were characterized by a combination of interfacial and cohesive fractures.

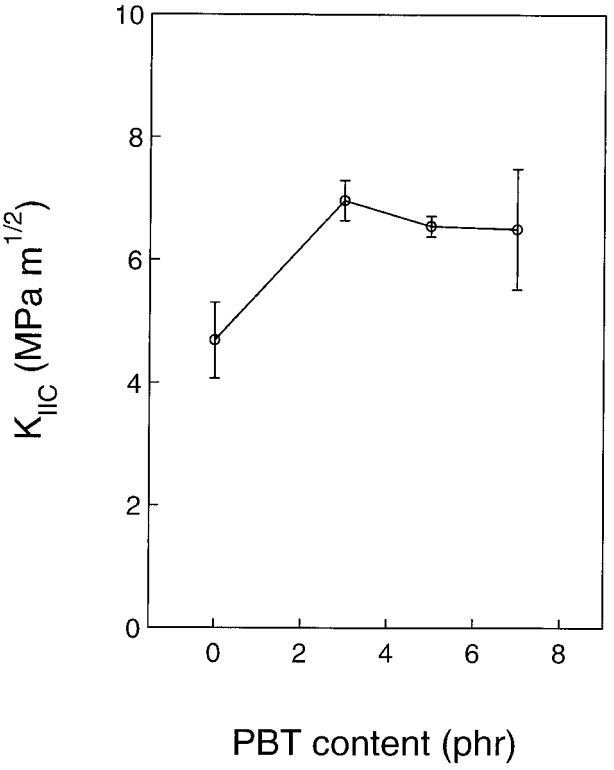

Figure 14 Mode II fracture toughness versus PBT content obtained from compact shear tests for layers of epoxy systems sandwiched between 6060-T5 aluminium adherends.

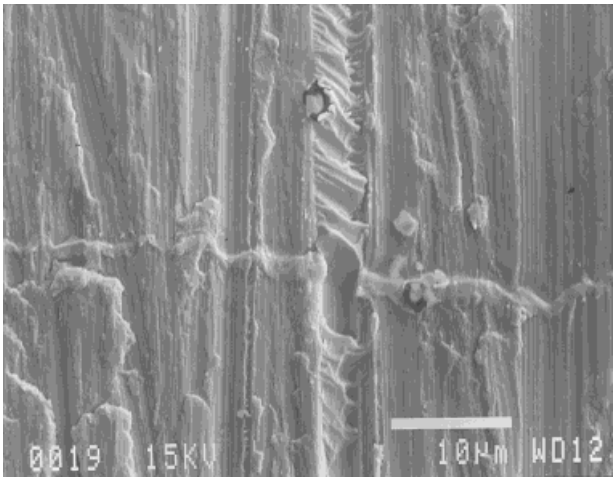

Figure 15 Control fracture surface of the adherend side of mode II compact shear specimen showing adhesive trapped in a valley longitudinally, and a strip of adhesive located horizontally in the middle is the mark of tunnelling of microcracks on adhesive side. The crack propagation direction is from top to bottom.

The fracture surfaces were examined using a SEM for more details. It was not unusual to observe localized cohesive failure mode in the visually interfacial fracture area. Figure 15 shows that the adherend side of the control has adhesive trapped in a valley longitudinally, and a strip of adhesive located horizontally in the middle is the mark left by tunnelling of microcracks on the adhesive side. Fracture surfaces of modified epoxy systems were, in general, composed of different patterns, including hackles, tunnelling, replica of adherend texture, and localized mode I microcracks. Figure 16(a) shows that the first 3 features occurred at a PBT content of 7 phr, and Figure 16(b) shows hackle marks at a higher magnification. Figure 16(c) shows that the localized mode I microcracks within an area of visually interfacial failure occurred at a PBT content of 3 phr, which are microscopically similar to hackle marks. The tunnelling of microcracks were often followed by interfacial fracture, as shown in Figure 16(a), the sequence of which was described elsewhere.[18] Also, it was observed that micro-

cracks leave marks made of adhesive on the other side of adherend, and, consequently, the failure mode in the area where microcracks exist is cohesive. Such an area includes that of hackle marks, tunnelling (Fig. 15), and localized microcracks. Anomalous behavior was noticed sometimes. For instance, the features of fracture surfaces in one bond line were found to be different from those in the other in the same specimen.

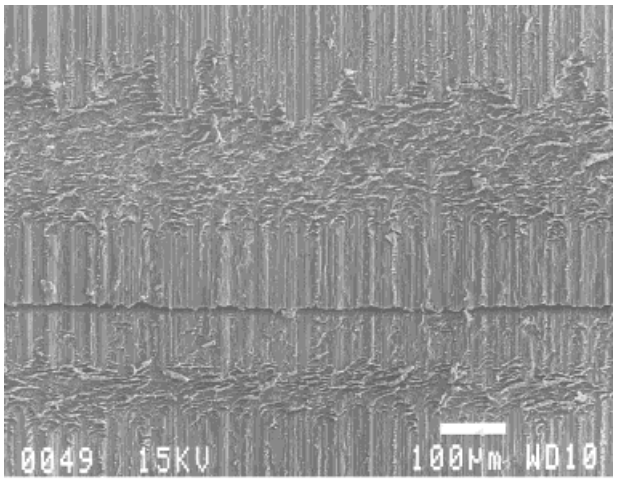

(a)

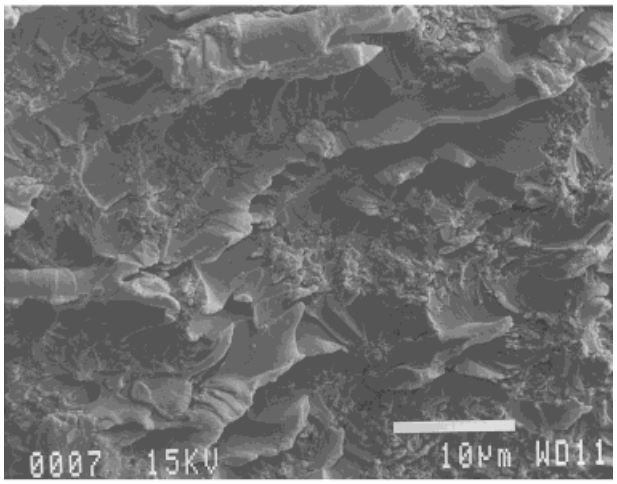

(b)

Figure 16 Morphological features of mode II fracture surface of adhesive side resulted from a compact shear specimen test for layers sandwiched between 6060-T5 aluminium adherends. The crack propagation direction is from top to bottom. From the top, the following is seen: (a) texture of adherend surface, hackle marks, texture of adherend surface, and tunnelling of microcracks at a PBT content of 7 phr; (b) hackle marks at a high magnification for a PBT content of 7 phr; and (c) localized microcracks within an area of interfacial fracture at a PBT content of 3 phr, which are microscopically similar to hackle marks.

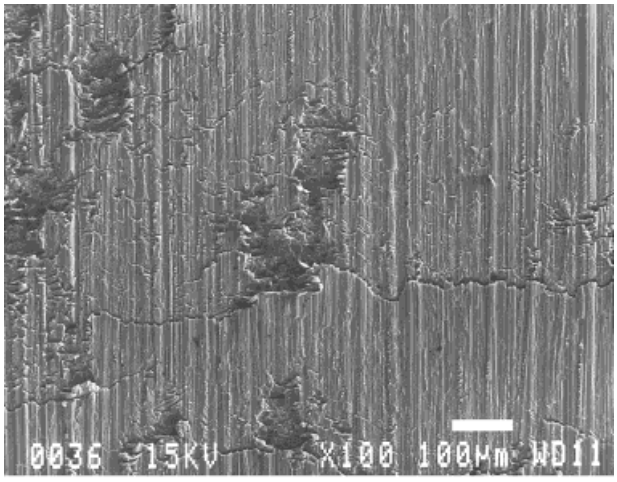

(c)

Figure 16 (*Continued*)

The increase in toughness of PBT-modified epoxy systems over the control seems to be due mainly to the hackle marks because (1) the hackle marks are the result of plastic deformation in a large area after microcracking, (2) tunnelling appears to be less deformed than hackle marks, which dominantly takes place in the control, and (3) the control seldom has hackle marks.

CONCLUSIONS

Mode II fracture of PBT-modified epoxy systems produced with a particular processing technique has been studied in comparison with mode I fracture. Increases in mode II fracture toughness of modified bulk epoxy systems over the control were found. It was deduced to account for the increases that PBT particles played a role of obstacles in mode II loading more than in mode I loading. In addition, fracture toughness of adhesive layers sandwiched between aluminium adherends under mode II loading was also found to increase with PBT modification. It was attempted to account for this increase using microscopic features.

REFERENCES

1. A. C. Garg and Y. W. Mai, *Compos. Sci. Technol.,* **31,** 179 (1988).
2. R. A. Pearson, in *Rubber-Toughened Plastics I—Science and Engineering,* Advances in Chemistry

Series 233, American Chemical Society, Washington, DC, 1993, p. 405.
3. J. K. Kim and R. E. Robertson, *J. Mater. Sci.,* **27,** 161 (1992).
4. D. Bhattacharjee and J. F. Knott, *Int. J. Fract.,* **72,** 359 (1995).
5. H. S. Kim and P. Ma, *Key Eng. Mat.,* **137,** 179 (1998).
6. D. Broek, *Elementary Engineering Fracture Mechanics,* Sijthoff & Noordhoff, 1978.
7. F. Erdogan and G. C. Sih, *J. Basic Eng.,* 519 (1963).
8. F. Ramsteiner, *Polymer,* **34,** 312 (1993).
9. M. E. Nichols and R. E. Robertson, *J. Polym. Sci., Part B: Polym. Phys.,* **32,** 1607 (1994).
10. G. G. Chell and E. Girvan, *Int. J. Fract.,* **14,** R81 (1978).
11. Y. W. Mai and A. S. Vipond, *J. Mater. Sci.,* **13,** 2280 (1978).
12. A. Anandarajah and A. E. Vardy, *J. Strain Anal.,* **19,** 173 (1984).
13. B. S. Oh, H. S. Kim, and P. Ma, in *Toughened Plastics II—Novel Approaches in Science and Engineering; Advances in Chemistry Series 252,* C. K. Riew and A. J. Kinloch, Eds., American Chemical Society, Washington, DC, 1996, p. 111.
14. H. S. Kim and P. Ma, *J. Appl. Polym. Sci.,* **61,** 659 (1996).
15. J. Kim and R. E. Robertson, in *Toughened Plastics I; Advances in Chemistry Series 233,* C. K. Riew and A. J. Kinloch, Eds., American Chemical Society, Washington, DC, 1993, p. 427.
16. F. F. Lange and K. C. Radford, *J. Mater. Sci.,* **6,** 1197 (1971).
17. M. E. Nichols and R. E. Robertson, *J. Mater. Sci.,* **29,** 5916 (1994).
18. H. Chai, *Int. J. Fract. Mech.,* **37,** 137 (1988).
19. Z. C. Xia and J. W. Hutchinson, *Int. J. Solids Struct.,* **31,** 1133 (1994).
20. W. L. Bradley, in *Application of Fracture Mechanics to Composite Materials,* K. Friedrich, Ed., Elsevier, New York, 1989, p. 159.
21. S. Ho and Z. Suo, *Trans. ASME,* **60,** 890 (1993).